

Biogeosciences Discussions is the access reviewed discussion forum of *Biogeosciences*

CO₂ budgeting at the regional scale using a Lagrangian experimental strategy and meso-scale modeling

C. Sarrat¹, J. Noilhan¹, P. Lacarrère¹, V. Masson¹, E. Ceschia², P. Ciais³,
A. Dolman⁴, J. Elbers⁵, C. Gerbig⁶, and N. Jarosz⁷

¹CNRM-GAME Météo France, 42 avenue Coriolis, 31057 Toulouse Cedex, France

²CESBIO, 18, avenue Edouard Belin 31401 Toulouse Cedex 9, France

³LSCE, CEA/Saclay, 91191 Gif-sur-Yvette Cedex, France

⁴Vrije Universiteit, De Boelelaan 1085, 1081 HV Amsterdam, The Netherlands

⁵ALTERRA, Droevendaalsesteeg 3, 6708 PB Wageningen, The Netherlands

⁶Max Planck Institute for Biogeochemistry, Hans-Knöll-Str. 10, 07745 Jena, Germany

⁷INRA, Avenue Edouard Bourlaux, B.P. 81 33883 Villenave d'Ornon, Cedex, France

Received: 22 May 2008 – Accepted: 28 June 2008 – Published: 23 July 2008

Correspondence to: C. Sarrat (claire.sarrat@cnrm.meteo.fr)

Published by Copernicus Publications on behalf of the European Geosciences Union.

2931

Abstract

An atmospheric Lagrangian experiment for regional CO₂ budgeting with aircraft measurements took place during the CarboEurope Regional Experiment campaign (CERES) in south-western France, in June, 2005. The atmospheric CO₂ aircraft measurements taken upstream and downstream of an active and homogeneous pine forest revealed a CO₂ depletion in the same air mass. This field experiment is analyzed with a meteorological meso-scale model interactively coupled with a surface scheme, allowing plant assimilation, ecosystem respiration, CO₂ anthropogenic emissions and sea fluxes. First, the model is carefully validated against observations close to the surface and in the atmospheric boundary layer. Then, the carbon budget is evaluated using the numerous CERES observations and as well as the modeling results in order to estimate the relative contribution of each physical process. A good agreement is shown in terms of the estimation of the regional CO₂ surface flux by the Eulerian meso-scale model budget and by the observations at the surface flux sites. A Lagrangian estimation of regional CO₂ surface flux from aircraft observations is more difficult due to several sources of uncertainty. In our case, probable errors are due to the determination of CO₂ vertical profile measurements and owing to the difficulties in monitoring the meteorological condition evolution during several hours.

1 Introduction

As the major greenhouse gas actor in climate change, a better knowledge of regional atmospheric CO₂ budget is needed, as well as an understanding of underlying processes. At the global and continental scale, models are able to infer the CO₂ surface fluxes (Bousquet et al., 1998), but the resolution of global inversions is too coarse to get accurate information at the regional scale. Meteorological meso-scale models permits the use of higher spatial resolution, better Atmospheric Boundary Layer (ABL) and surface energy budget parametrizations and the explicit resolution of local to re-

2932

gional wind circulations that are crucial for the understanding of the atmospheric CO₂ variability (Pérez-Landa et al., 2007). Previous studies (Sarrat et al., 2007a; Sarrat et al., 2007b; Nicholls et al., 2004; Denning et al., 2003) showed the good capacity of meso-scale models to simulate the CO₂ surface fluxes as well as the atmospheric concentration gradients and their variability. In this paper, we use regional modeling and experimental data from the CarboEurope Regional Experiment Strategy (CERES) campaign (Dolman et al., 2006) to estimate the CO₂ uptake fluxes during daytime, over a flat and homogeneous active forest, surrounded by an agricultural area. A specific Lagrangian experiment was conducted in June 2005, during a westerly wind episode, over the Landes forest, south-western France (Fig. 1). The Lagrangian sampling strategy consisted in following an oceanic air mass moving towards land and sampling it, first above the ocean, then over the active forest and then again further downstream of the forest, knowing the wind speed and the time needed for the air mass to be advected. The measured CO₂ decrease between upstream and downstream of the forest is related to the CO₂ uptake. Lagrangian aircraft experiments have recently been established as a method to measure regional scale trace gas fluxes (Lin et al., 2004; Lin et al., 2006; Lin et al., 2007; Matross et al., 2006). Schmitgen et al., 2004 already showed the potential of a Lagrangian budgeting approach for accurately estimating CO₂ fluxes for the Landes region. In this study, both experimental data and a meteorological meso-scale model at high resolution are used. After a description of the experimental and modeling tools, the simulation outputs are compared to several types of observations. Then, we analyze the CO₂ regional budget using both the modeling results and the Lagrangian experiment, in order to quantify the regional CO₂ fluxes.

2933

2 Method to estimate CO₂ budget at the regional scale

2.1 The Lagrangian Experiment

The May–June 2005 CERES experiment was performed in south-western of France, as shown in Fig. 1a. The area contains a large and rather homogeneous pine forest bounded by the Atlantic ocean to the west and an agricultural area to the east. The experimental set-up, described by Dolman et al. (2006) included 10 surface fluxes stations, located on ecosystems representative of the region (vineyards, maize, wheat, pine forest...). In the pine forest, the evolution of the Atmospheric Boundary Layer (ABL) was monitored at La Cape Sud (noted LACS in Fig. 1b) with radio-soundings, a UHF radar, meteorological and flux measurements. The vertical and horizontal variations of CO₂ concentration were sampled by four research aircraft and two towers (in Biscarosse and Marmande, respectively noted BISC and MARM in Fig. 1b). More details on the experimental strategy can be found in Dolman et al. (2006). A Lagrangian experiment was performed on the 6 June 2005. The north-west wind was regular all day, with a speed of nearly 6.5 m s⁻¹ in the ABL and which was spatially homogeneous. Only few clouds were observed near the Atlantic coast, elsewhere the sky was clear and the temperature reached 25°23C. In the morning, the air mass was sampled by the Piper-Aztec aircraft, close to the Atlantic coast (Transect A, as shown in Fig. 1b). The same air mass was sampled once again (Transect B), a few hours later over land. Two special constant volume balloons were launched from Cape Sud to sample the temperature and moisture in a truly Lagrangian fashion at fixed density levels. Information on the wind patterns and flight paths of the balloons were transmitted to the pilot of the aircraft in order to help them fly in a Lagrangian sampling mode.

2.2 Meso-scale modeling with Meso-NH

This Lagrangian experiment day is simulated using the meteorological model, Meso-NH, a non-hydrostatic meso-scale model (Bélair et al., 1998). The model is run with

2934

two domains (two-ways nesting mode) allowing a high resolution of 2 km for the inner domain displayed in Fig. 1b, and a 10 km resolution for the larger one (domain width 900 km×900 km, not shown here). The atmospheric Meso-NH model includes the CO₂ concentration, transported as a passive scalar. The surface energy and CO₂ fluxes are computed on-line by the surface scheme, ISBA-A-gs (Noilhan and Planton, 1989; Calvet et al., 1998), including CO₂ assimilation by the vegetation and ecosystem respiration. In the surface scheme, the latent heat flux as well as the carbon flux are computed through the stomatal conductance. The land cover is from an improvement of the Ecoclimap database at 1 km resolution (Champeaux et al., 2005; Masson et al., 2003) and contains 62 types of cover. For the natural surface (i.e. all surface types but town, sea and lake), a tile approach is used in ISBA-A-gs, in which each 2 km grid cell is divided into patches (bare soil, snow, rock, tree, coniferous, evergreen, C3 crops, C4 crops, irrigated crops, grassland tropical grasslands and parks). The energy and CO₂ budgets are calculated for each patch within each grid cell and then averaged at the grid scale, according the areal fraction of each patch. The anthropogenic CO₂ emissions are provided by the 10 km inventory of the Stuttgart University (Dolman et al., 2006). An oceanic CO₂ fluxes are parametrized according to Takahashi et al. (1997). The simulation is initialized at 18:00 UTC on the 5 June, using the European Centre for Medium-Range Weather Forecasts (ECMWF) analysis, for both the surface and the meteorological fields and runs for 30 h. The meteorological lateral boundary conditions are forced every six hours with the ECMWF analysis. The CO₂ concentration are initialized with a homogeneous vertical profile over the whole domain, while a zero horizontal concentration gradient is applied at the boundaries of the larger scale domain.

2.3 Three methods for estimating the CO₂ budget

In order to establish as accurately as possible, the regional CO₂ budget, we use both the meso-scale modeling results and the set of observations made during the Lagrangian experiment. The estimation of the CO₂ budget is based on the resolution

2935

of the equation of the CO₂ temporal evolution decomposed into three terms:

$$\frac{\partial \text{CO}_2}{\partial t} = -\bar{u} \frac{\partial \text{CO}_2}{\partial x} - \bar{v} \frac{\partial \text{CO}_2}{\partial y} - \frac{\partial \overline{w' \text{CO}_2'}}{\partial z} \quad (1)$$

Where $\overline{w' \text{CO}_2'}$ is the vertical turbulent flux of CO₂, \bar{u} and \bar{v} the mean horizontal wind components. We test three methods to determine the regional CO₂ budget, based on the two aircraft measurements (Dimona and Piper-Aztec described before):

1. After validation, the Meso-NH model is used to estimate the contribution of each transport term, giving a numerical Eulerian budget (Sect. 3.2);
2. The observations from the flux site network are used to calculate an average regional “bottom-up” flux using a simple averaging based upon the fractional coverage of each ecosystem (Sect. 3.3);
3. The Lagrangian budget is estimated using the aircraft observations (Sect. 3.4).

For each of the two aircraft experiments described in Sect. 3.1.4, the Dimona and the Piper-Aztec flights, we determine a sub-domain corresponding to the aircraft trajectories. In these sub-domains, the CO₂ surface fluxes are evaluated using the 3 methods.

3 Results

3.1 Comparisons of model and observations

In order to validate the simulation, the Meso-NH outputs are compared with the several types of observations made during CERES. The ABL height and structure are analysed, the CO₂ surface fluxes for 6 different cover types as well as the CO₂ concentration near the coast and in the agricultural zones are compared with the in-situ observations. Finally, the observations of CO₂ concentration made during the Lagrangian flights within the ABL are compared with the model outputs.

2936

3.1.1 Atmospheric boundary layer

During the CERES Intensive Observation Period (IOP), radio-soundings (RS) were launched every 3 hours at the central forest site LACS. The Fig. 2 shows an evaluation of the simulated ABL height compared with the RS launched during the early morning, at 05:00 UTC and at 17:00 UTC. This figure compares the vertical profiles of the potential temperature (left) and of the mixing ratio (right). At 05:00 UTC, the stable ABL is well simulated by the model, even if the mixing ratio is underestimated: the vertical structure within the first 2000 m is in good agreement with the observations. At 17:00 UTC, the potential temperature is slightly underestimated at the top of the ABL, but the vertical profile of the mixing ratio shows that the simulated ABL height is at almost 1100 m, in agreement with the observations. During the day, the humidity in the ABL increases and reaches 9 g kg^{-1} , due to the evapotranspiration and the moisture advection from the sea.

3.1.2 CO₂ surface fluxes

The diurnal cycles of the measured CO₂ fluxes are compared with the simulated values in Fig. 3 at several surface stations with various vegetation cover types: rapeseed, wheat, pine forest, vineyard and maize. The flux sites were selected to be representative of the main land cover types of the area. In general, the model is in good agreement with the CO₂ observations, the nocturnal respiration and the diurnal NEE (Net Ecosystem Exchange). At this time of the year, the winter crops (as rapeseed and wheat) assimilate carbon at almost their maximal rates (up to $25 \mu \text{ mol m}^{-2} \text{ s}^{-1}$), as well as the pine forest. Even if the assimilation differs from one maize site, to the other, the model is able to simulate both of them correctly, mainly because the LAI field prescribed in the meso-scale model has a good level of realism. When comparing the model with observations of latent and sensible heat fluxes (not shown here), a weaker agreement is found than for CO₂ fluxes.

2937

3.1.3 CO₂ concentration at the tower sites

The observed CO₂ concentration at the BISC and MARM sites are compared to the simulated concentration in Fig. 4. Even if the CO₂ concentration are slightly overestimated at night at BISC (left panel), the simulated concentration after 06:00 UTC are in good agreement with the observations. These comparisons show that the CO₂ inflow is steady state and regular all day. At MARM (right panel), the nocturnal maximum due to the ecosystem respiration is underestimated by the model. In fact, the first level of the model is at 20 m height, while the surface measurements are representative of the ground concentration. The daily concentration are better represented by the model, when the diurnal mixing occurs. The difference in concentration for both the observed and the modeled and between the ocean and the agricultural areas during the afternoon is approximatively 4 to 6 ppm.

3.1.4 Aircraft in-situ measurements

During this IOP day, several measurement flights have been operated, over the Landes forest. The MetAir Dimona aircraft (<http://www.metair.ch>) measured CO₂ at 1 Hz with an accuracy of better than 0.5 ppm using a combination of open and closed path sensors, as well as flask analysis (Dolman et al., 2006), along a trajectory following the air mass for over 3 h which is displayed in Fig. 5a. The aircraft trajectory is simulated on-line in the model, which means that, the CO₂ in the model is interpolated in space and time to the exact location of the aircraft trajectory. The comparison between the CO₂ observed by the Dimona and the simulation (Fig. 5b) shows the good ability of the model to reproduce slight concentration variabilities in and above the ABL, in the morning and the early afternoon, due to the vertical mixing and the CO₂ assimilation by the vegetation. The model also reproduces the slow decrease of CO₂ concentration from the morning to the time at the end of the flight. A second aircraft, the Météo France Piper-Aztec, flew over the ocean in the morning (red trajectory in Fig. 1b) and then downstream to the Landes forest in the afternoon (green trajectory in Fig. 1b), for

2938

the so-called “Lagrangian Experiment”, described in Sect. 2.1. The Fig. 6 shows the variation of CO₂ concentration between the transects A and B, observed by the aircraft measurements. In fact, the CO₂ time series show that during the morning flight, over the ocean and the forest area, the CO₂ concentration are constant with time and space: between 382 and 383 ppm in and above the ABL (Fig. 6a). During the afternoon flight, the CO₂ concentration are lower in the ABL and remain close to 382 ppm above it (Fig. 6b). Therefore, in the same air mass, the CO₂ depletion in the ABL upstream and downstream the pine forest is measured to be 4 to 6 ppm. The CO₂ concentration simulated by Meso-NH are in good agreement with these observations even if slight discrepancies occur at low altitudes.

The model outputs have been compared reasonably well with several types of observations (air temperature, wind speed, surface energy fluxes), but these comparisons are not shown here. Moreover, previous studies (Sarrat et al., 2007a,b) showed the good ability of the model to reproduce the energy surface fluxes as well as the meso-scale circulations on the 27 May and 6 June, during CERES.

3.2 Numerical Eulerian budget from Meso-NH

The Meso-NH model calculates the contribution of each term corresponding to the right-hand side of the Eq. 1. In order to facilitate the analysis, the simulated budget terms are designated in the following as:

- the total advective tendency: $ADV = -\bar{u} \frac{\partial CO_2}{\partial x} - \bar{v} \frac{\partial CO_2}{\partial y}$,
- the turbulent tendency: $TURB = -\frac{\partial \overline{w'CO_2'}}{\partial z}$.

It remains: $\frac{\partial CO_2}{\partial t} = ADV + TURB$ The numerical budget terms are calculated separately for the two Lagrangian experiments, of the Piper-Aztec and the Dimona flights over their respective sub-domains. For the Dimona, the budget terms are integrated over the 3 h of the flight, between 10:00 and 13:00 UTC, over a sub-domain encompassing the aircraft trajectory (hereafter called the Dimona box, represented in Fig. 5a).

2939

The Fig. 7a represents the simulated CO₂ vertical profiles at 10:00 (black) and 13:00 UTC (green) averaged over the Dimona box, while the Fig. 7b represents the horizontally averaged budget terms. Near, the surface, the turbulent flux due to assimilation is compensated by the advection of CO₂-rich oceanic air. At the top of the boundary layer, the turbulent flux is negligible. Integrating the turbulent tendency $TURB = -\frac{\partial \overline{w'CO_2'}}{\partial z}$, from the surface up to the ABL top gives the mean surface flux calculated by the model, $\overline{w'CO_2'}_{BUDGET} = -11.5 \mu\text{mol m}^{-2} \text{s}^{-1}$.

The equivalent integration is done for the Piper-Aztec flights, between 08:00 and 17:00 UTC and then averaged over the horizontal sub-domain (hereafter called the Piper box, displayed in Fig. 1b). The Fig. 7c represents the averaged vertical profiles of CO₂ concentration over the Piper box at 08:00 (black) and 17:00 UTC (green). The morning profile presents an accumulation of CO₂ near the surface due to the ecosystem respiration within the nocturnal stable ABL. At 17:00 UTC, the CO₂ depletion is very important near the surface (6 ppm) and varies between 2 and 6 ppm in the mixed ABL. This is in good agreement with the depletion observed by the Piper-Aztec aircraft during the Lagrangian flights (Fig. 6). Figure 7d represents the vertical profiles of the advective (red) and turbulent (green) CO₂ tendencies, averaged between 08:00 and 17:00 UTC over the Piper box. The advective term tends to provide oceanic air which is higher in CO₂ than the ABL exposed to forest uptake. This enrichment is compensated by the turbulent tendency (corresponding to the assimilation by the vegetation and the vertical mixing) which decreases the CO₂ in the layer especially near the surface. At the top of the ABL, the simulated entrainment flux is once again negligible. If we examine the budget term at the first level of the model, the net difference between 08:00 and 17:00 UTC is –6 ppm due to:

- the advection up to 13 ppm from oceanic CO₂-rich air.
- a turbulent contribution, dominated by plant assimilation and resulting in a CO₂ variation that reaches –15 ppm near the surface.

- The integration over the ABL of the turbulent flux gives $\overline{w'CO_2'}_{2BUDGET} = -10.4 \mu\text{mol m}^{-2} \text{s}^{-1}$.

The anthropogenic emissions represent less than 2% of the total CO_2 fluxes at the surface, they are negligible, when averaged over the Piper or Dimona boxes.

5 3.3 CO_2 area-average surface fluxes from in-situ measurements

A second way to estimate the CO_2 surface fluxes over the region is to use the continuous flux observations at eddy covariance stations distributed in the area (Fig. 1a). In fact, the surface station network is assumed to be dense enough during CERES to have a representative sample of the land cover and to upscale the net ecosystem exchange of the domain. The Table 1 lists the different flux stations and the fraction of the corresponding type of cover in the respective sub-domains. These proportions are deduced from the Ecoclimap land cover database.

The weighted observed fluxes are integrated between 10:00 and 13:00 UTC for the Dimona sub-domain, which is dominated by pine forest (68% of the box). In the Dimona box, the weighted surface flux is $\sum_i^{\text{obs}} \overline{w'CO_{2i}'} = -12.1 \mu\text{mol m}^{-2} \text{s}^{-1}$. This value is in good agreement with the model Eulerian budget. For the Piper-Aztec sub-domain, the mean fluxes are calculated between 08:00 and 17:00 UTC. In this box, the weighted surface flux is $\sum_i^{\text{obs}} \overline{w'CO_{2i}'} = -9.4 \mu\text{mol m}^{-2} \text{s}^{-1}$, a value slightly lower than the model Eulerian budget. The weighted CO_2 flux over the Dimona sub-domain is logically higher than the flux over the Piper-Aztec sub-domain, because the hours of integration around noon are the most favourable for the photosynthetic activity. Moreover, the Dimona box is dominated by the pine forest which is relatively active at this time of the year.

2941

3.4 Lagrangian budgeting

The third way to establish a regional budget is to use the aircraft observations. Integrating the Eq. 1 between the surface and above the ABL height (z_i) leads to:

$$\int_0^{z_i} \frac{\partial \text{CO}_2}{\partial t} dz = -[\overline{w'CO_{2\text{ent}}'} - \overline{w'CO_{2\text{surf}}'}] \quad (2)$$

5 Where $\overline{w'CO_{2\text{ent}}'}$, the entrainment CO_2 flux is negligible above the ABL, z_i . As we consider the same air mass during its displacement, the advection is neglected. We can deduce from Eq. 2, the CO_2 flux at the surface, $\overline{w'CO_{2\text{surf}}'}$.

The $\text{LAG}_{\text{obs}} = \int_0^{z_i} \frac{\partial \text{CO}_2}{\partial t} dz$ corresponds to the variation of CO_2 into the same air mass observed during the morning flights near the coast line and the observations made in the afternoon further inland, for the two aircraft. In these conditions, the CO_2 surface flux can be approximated by integrating the variation of the CO_2 vertical profiles in the ABL between the morning and the afternoon measurements. The vertical profiles of observed CO_2 concentration displayed in Fig. 8 for the 2 aircraft, are integrated up to the top of the ABL. For the Dimona measurements, we assume, that the CO_2 concentration are well mixed in the ABL. The mean depletion of CO_2 in the ABL between 10:00 and 13:00 UTC is almost 3 ppm. The integration up to 1600m gives: $\text{LAG}_{\text{obs}} = -16.8 \mu\text{mol m}^{-2} \text{s}^{-1}$. The Piper-Aztec measurements show a well mixed layer in the morning and a larger depletion of more than 5 ppm over the nine hours of the experiment. The observations near the surface for the afternoon flight are interpolated. 20 The integration of the variation between the two vertical profiles, up to 2000 m gives: $\text{LAG}_{\text{obs}} = -8.6 \mu\text{mol m}^{-2} \text{s}^{-1}$.

4 Discussion

Three methods to establish a regional CO_2 budget have been tested using observations and model outputs analysis. The Table 2 summarizes the results obtained by

2942

these methods for two sub-regions. The CO_2 surface fluxes obtained by the three methods vary between 10 and $16 \mu\text{mol m}^{-2} \text{s}^{-1}$, values lower than the fluxes retrieved by Gibert et al. (2007), over a region dominated by winter crops in May or by Schmitgen et al. (2004), in the Landes in June, respectively of 20 and $16 \mu\text{mol m}^{-2} \text{s}^{-1}$.

5 The budgets calculated according the Dimona measurements and sub-domain are higher than the Piper-Aztec ones, using the 3 methods. The main reason is that the time of integration is shorter and centered over the maximum of assimilation for the Dimona box. Moreover, this sub-domain is smaller and mainly covered by the pine forest (68%). For this ecosystem, the assimilation rate is high at this stage of the year. The averaged surface fluxes obtained from surface observation and from the meso-scale model are in good agreement for the two boxes. This confirms the good calibration of the ISBA-A-gs surface scheme and the fair quality of the meso-scale circulations representation in the model. Moreover, in general, the model is able to reproduce the surface fluxes and the CO_2 concentration observed by the aircraft. The high level of realism of the Meso-NH simulation gives confidence to the estimation of the Eulerian budget. Indeed the Meso-NH budget calculation shows that the contribution of carbon assimilation by the vegetation is higher than the advection of CO_2 into the domain in both aircraft boxes allowing the diurnal CO_2 decrease in the ABL. The interpretation of the results obtained with the Lagrangian aircraft budgeting is more complex. For the Dimona box, the Lagrangian budget leads to a higher surface flux than the two other methods. A reverse result is obtained in the Piper-Aztec box. Various explanations can be proposed:

- First, while the morning profiles of CO_2 flown over the sea are comparable for the two aircraft, the afternoon ones are incomplete in both cases, particularly in the lowest layer. The two inland profiles have been extrapolated in the lowest layers. This could introduce uncertainties in the estimation of the Lagrangian term.
- Secondly, even if we tried as much as possible to plan the afternoon aircraft flights in order to follow and to sample the same air mass than during the morning flight,

2943

in agreement with wind observations, uncertainties cannot be avoided. For instance, variations of the wind field within the meso-scale domain are difficult to be taken into account in the forecast of the air mass trajectory.

5 Conclusions

5 This paper correspond to a validation of a meso-scale model able to calculate the regional CO_2 budgets, due to the full interaction of water and carbon exchanges between the surface and the atmosphere. The Lagrangian experiment conducted during the CERES campaign over a coniferous forest is simulated with a meso-scale meteorological model. During a westerly wind episode, an oceanic air mass has been sampled twice in the morning, near the Atlantic ocean coast line and further inland several hours later. This experiment has been conducted twice. For the Dimona aircraft, between the morning and the afternoon measurements, the air mass CO_2 concentration have decreased by almost 3 ppm in 3 h. For the Piper-Aztec aircraft, the decrease reached 5 to 6 ppm. The meso-scale model is first evaluated against radio-sounding, CO_2 surface flux observations, CO_2 measurements at 2 sites and CO_2 concentration from the aircraft observations. The comparisons show that the model is able to reproduce correctly both the ABL development and the CO_2 mixing ratio in and above the ABL as well as the NEE. Next, three methods are tested to determine the regional CO_2 surface flux: the numerical model budget calculation using an Eulerian method, the surface flux station observations and the Lagrangian observations by aircraft. All of the budgets are in good agreement as displayed in Table 2. The regional surface flux is between -10 and $-16 \mu\text{mol m}^{-2} \text{s}^{-1}$ depending on the time of integration and the areas considered. More specifically, the estimations of the regional CO_2 surface flux by the Eulerian meso-scale model budgeting and by the observations at the surface flux sites are very close. The Lagrangian estimation of regional CO_2 surface flux from aircraft observations is more difficult due to uncertainties. In our case, probable errors are due to the determination of CO_2 vertical profile measurements and to the difficulties in monitoring

2944

the meteorological condition evolution during several hours. The CERES database offers the opportunity to perform similar study for a large number of cases with different environmental conditions encountered during the Spring and Autumn 2007 campaigns.

Acknowledgements. The authors would like to thank all CarboEurope partners who made CERES a very successful experiment. We especially would like to thank Pierre Durand for his contribution in the coordination of the campaign, G. Facon for operating the drifting balloons system. Many thanks also to Sylvie Donier for her continuous assistance in the modeling work and to Marc Pontaud and the SAFIRE team who operated the Piper-Aztec. Support for flying the Piper-Aztec was mainly provided by CNES, CNRS-INSU, Météo France. Thanks to A. Boone who carefully checked the English quality.

References

- Bélaïr, S., P. Lacarrère, J. Noilhan, V. Masson, and J. Stein, High-resolution simulation of surface and turbulent fluxes during HAPEX-MOBILHY, *Mon. Wea. Rev.*, 126, 2234–2253, 1998. 2934
 - 15 Bousquet, P., P. Ciais, P. Monfray, Y. Balkanski, M. Ramonet, and P. Tans, Influence of two atmospheric transport models on inferring sources and sinks of atmospheric CO₂, *Tellus*, 48B, 568–582, 1998. 2932
 - Calvet, J.-C., J. Noilhan, J.-L. Roujean, P. Bessemoulin, M. Cabelguenne, A. Olioso, and J.-P. Wigneron, An interactive vegetation SVAT model tested against data from six contrasting sites, *Agri. For. Meteorol.*, 92, 73–95, 1998. 2935
 - 20 Champeaux, J., H. Fortin, and K.-S. Han, Spatio-temporal characterization of biomes over south-west of France using SPOT/VEGETATION and Corine Land Cover datasets, *IGARSS'05 Proceedings*, 2005. 2935
 - Denning, S., M. Nicholls, L. Prihodko, I. Baker, P.-L. Vidale, K. Davis, and P. Bakwin, Simulated variations in atmospheric CO₂ over a Wisconsin forest using a coupled ecosystem-atmosphere model, *Glob. Change Biol.*, 9, 1241–1250, 2003. 2933
 - 25 Dolman, A., J. Noilhan, P. Durand, C. Sarrat, A. Brut, A. Butet, N. Jarosz, Y. Brunet, D. Loustau, E. Lamaud, L. Tolk, R. Ronda, F. Miglietta, B. Gioli, E. Magliulo, M. Esposito, C. Gerbig, S. Krner, P. Galdemard, M. Ramonet, P. Ciais, B. Neininger, R. Hutjes, J. Elbers, T. Warnecke, G. Landa, M. Sanz, Y. Scholz, and G. Facon, CERES, the CarboEurope Regional 2945
-
- Experiment Strategy in Les Landes, south-west France, May–June 2005, *BAMS*, 87(10), 1367–1379, 2006. 2933, 2934, 2935
 - Gibert, F., M. Schmidt, J. Cuesta, P. Ciais, M. Ramonet, I. Xueref, E. Larmanou, and P.H. Flamant, Retrieval of average CO₂ fluxes by combining in situ CO₂ measurements and backscatter lidar information, *J. Geophys. Res.*, 112, D10301, doi:10.1029/2006JD008190, 2007.
 - 5 Lin, J., C. Gerbig, S. Wofsy, A. Andrews, B. Daube, C. Grainger, B. Stephens, P. Bakwin, and D. Hollinger, Measuring fluxes of trace gases at regional scales by Lagrangian observations: Application to the CO₂ budget and rectification airborne (COBRA) study, *Journal of Geophysical Research*, 109(D15), D15304, doi:10.1029/2004JD004754, 2004. 2933
 - 10 Lin, J. C., C. Gerbig, S. C. Wofsy, B. C. Daube, D. M. Matross, V. Y. Chow, E. Gottlieb, A. E. Andrews, M. Pathmathevan, and J. W. Munger, What have we learned from intensive atmospheric sampling field programs of CO₂?, *Tellus Series B*, 58(5), 331–343, 2006. 2933
 - 15 Lin, J. C., C. Gerbig, S. C. Wofsy, V. Y. Chow, E. Gottlieb, B. C. Daube, and D. M. Matross, Designing Lagrangian experiments to measure regional-scale trace gas fluxes, *J. Geophys. Res.*, 112, D13312, doi:10.1029/2006JD008077, 2007. 2933
 - Masson, V., J. Champeaux, F. Chauvin, C. Mériquet, and R. Lacaze, A global database of land surface parameters at 1 km resolution for use in meteorological and climate models, *J. Climate*, 16, 1261–1282, 2003. 2935
 - 20 Matross, D. M., A. E. Andrews, M. Pathmathevan, C. Gerbig, J. C. Lin, S. C. Wofsy, B. C. Daube, E. W. Gottlieb, V. Y. Chow, J. T. Lee, C. Zhao, P. S. Bakwin, J. W. Munger, and D. Y. Hollinger, Estimating regional carbon exchange in New England and Quebec by combining atmospheric, ground-based and satellite data, *Tellus*, 58B, 344–358, 2006. 2933
 - Nicholls, M., S. D. et L. Prihodko, P.-L. Vidale, I. Baker, K. Davis, and P. Bakwin, A multiple-scale simulation of variations in atmospheric carbon dioxide using a coupled biosphere-atmospheric model, *J. Geophys. Res.*, 109(D18), D18117, doi:10.1029/2003JD004482, 2004. 2933
 - Noilhan, J. and S. Planton, A simple parametrization of land surface processes for meteorological models, *Mon. Wea. Rev.*, 117, 536–549, 1989. 2935
 - 30 Pérez-Landa, G., P. Ciais, G. Gangoiti, J. Palau, A. Carrara, B. Gioli, F. Miglietta, M. Schumacher, M. Millan, and J. Sanz, Mesoscale circulations over complex terrain in the Valencia coastal region, Spain - part 2: Modeling CO₂ transport using idealized surface fluxes, *Atmos. Chem. Phys.*, 7, 1851–1868, 2007. 2933

- Sarrat, C., J. Noilhan, A. Dolman, C. Gerbig, R. Ahmadov, L. Tolk, A. Meesters, R. Hutjes, H. T. Maat, G. Pèrez-Landa, and S. Donier, Atmospheric CO₂ modeling at the regional scale: An intercomparison of 5 meso-scale atmospheric models, *Biogeosciences*, 4, 1115–1126, 2007a. 2933, 2939
- 5 Sarrat, C., J. Noilhan, P. Lacarrère, S. Donier, C. Lac, J.-C. Calvet, A. Dolman, C. Gerbig, B. Neininger, P. Ciais, J. Paris, F. Boumard, M. Ramonet, and A. Butet, Atmospheric CO₂ modeling at the regional scale : Application to the CarboEurope Regional Experiment, *J. Geophys. Res.*, 112, D12105, doi:10.1029/2006JD008107, 2007b. 2933, 2939
- Schmitgen, S., H. Gei, P. Ciais, B. Neininger, Y. Brunet, M. Reichstein, D. Kley, and A. Volz-Thomas, Carbon dioxide uptake of a forested region in southwest France derived from airborne CO₂ and CO measurements in a quasi-Lagrangian experiment, *J. Geophys. Res.*, 109(D14), D14302, doi:10.1029/2003JD004335, 2004. 2933
- 10 Takahashi, T., R. Feely, R. W. ans R. Wanninkhof, D. Chipman, S. Sutherland, and T. Takahashi, Global air-sea flux of CO₂ : An estimate based on measurements of sea-air pCO₂ difference, *Proc. Natl. Acad.*, 94, 8292–8299, 1997. 2935
- 15 Tennekes, H., A model for the dynamics of the inversion above a convective boundary layer, *J. of Atm. Sci.*, 30, 558–567, 1973.
- Vilà-Guerau, J., B. Gioli, F. Miglietta, H. Jonker, H. Baltink, R. Hutjes, and A. Holtslag, Entrainment process of carbon dioxide in the atmospheric boundary layer, *J. Geophys. Res.*, 109(D18), D18110, doi:10.1029/2004JD004725, 2004.
- 20

2947

Table 1. Weighting of the CO₂ surface fluxes between 08:00 and 17:00 UTC and between 10:00 and 13:00 UTC ($\mu\text{mol m}^{-2} \text{s}^{-1}$) observed at several CERES stations. The vegetation type percentage in the 2 boxes are deduced from the Ecoclimap database. The bare soil corresponds to 4 to 5% of each box.

Representative station	Type of vegetation					Weighted total flux $\sum_i^{\text{obs}} C_i w_i \overline{\text{CO}_2'}_{P_i}$ $\mu\text{mol m}^{-2} \text{s}^{-1}$
	Tree Cauhins	Coniferous Le Bray	C3 crops Cape Sud beans Auradé Lamasquère	C4 crops Cape Sud maize Marmande	Grass Le Fauga	
Mean CO ₂ flux 10:00–13:00 UTC	–7.4	–14.3	–11.2	–11.8	–4.3	–12.1
Mean CO ₂ flux 08:00–17:00 UTC	–6.5	–11.8	–10.2	–10.9	–3.0	–9.4
Percent of the DIMONA box	10	68	4	5	3	
Percent of the PIPER box	18	51	7	6	7	

2948

Table 2. CO₂ budget calculated according 3 methods (in $\mu\text{mol m}^{-2} \text{s}^{-1}$). The Eulerian budget is calculated with the Meso-NH model, the Observed surface flux budget is deduced from the area-average CO₂ surface flux measurements (Table 1) and the Lagrangian budget (LAG_{obs}) is deduced from the aircraft vertical profile measurements during experiment. Each budget is averaged over the Piper and the Dimona sub-domains.

Time of integration		Eulerian budget	Observed surface fluxes	LAG _{obs}
		MODEL	$\sum_i^{\text{obs}} C_i w' \overline{\text{CO}_{2i}}$	$\overline{w' \text{CO}_{2\text{LAG}}}$
DIMONA	3 h	−11.5	−12.1	−16.8
PIPER	9 h	−10.4	−9.4	−8.6

2949

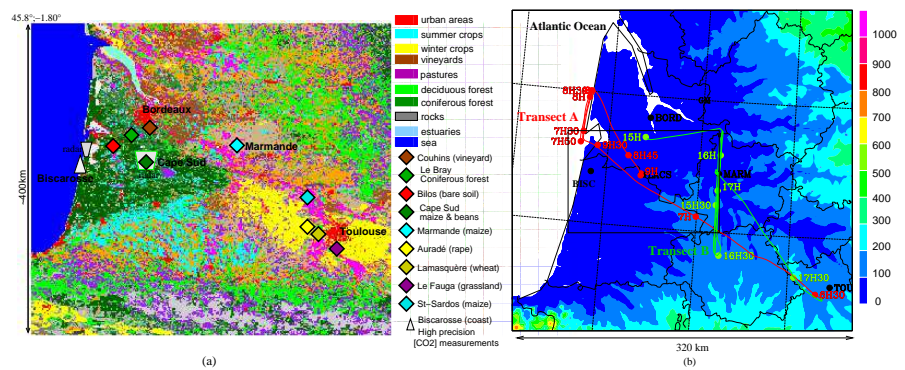


Fig. 1. (a) Experimental set-up during CERES; **(b)** Altitude (m), aircraft trajectories and budget calculation sub-domain.

2950

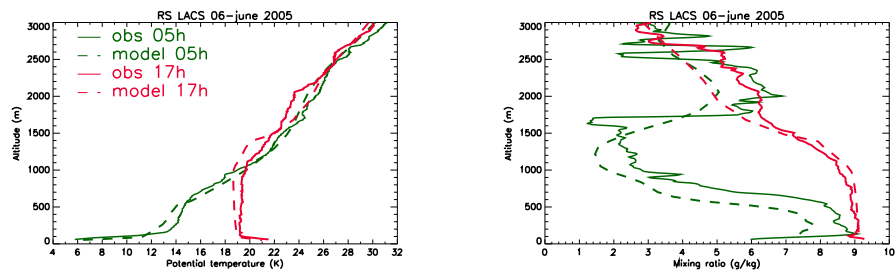


Fig. 2. Potential temperature ($^{\circ}\text{C}$) (left) and mixing ratio (right) observed and simulated in the forest central site La Cape Sud at 05:00 UTC (green) and 17:00 UTC (red).

2951

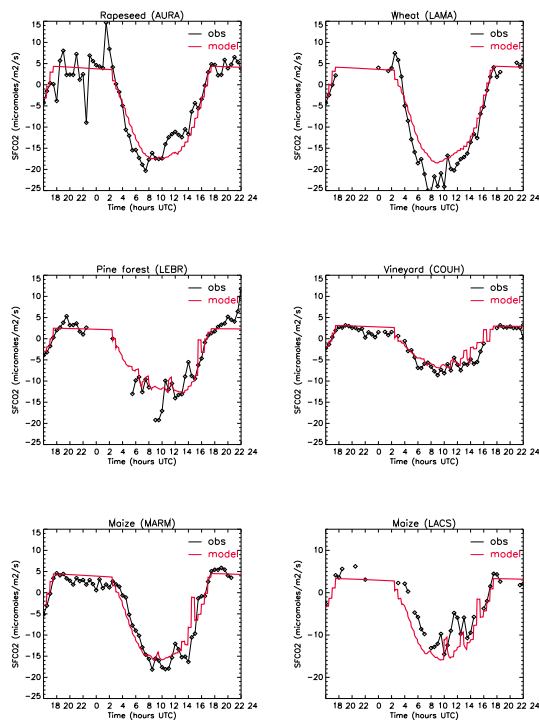


Fig. 3. Comparisons of CO_2 surface fluxes ($\mu\text{mol m}^{-2} \text{s}^{-1}$) at several surface stations: observations (black), model (red).

2952

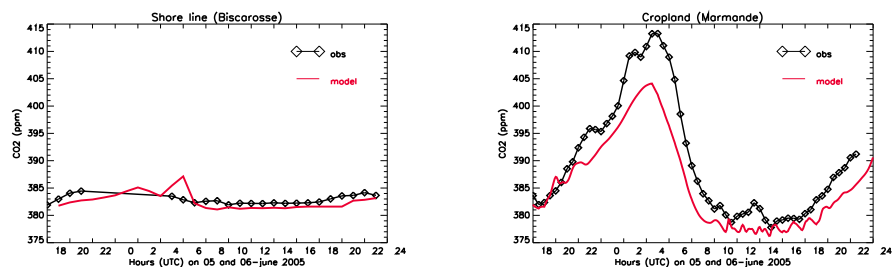


Fig. 4. CO₂ concentration simulated and observed in BISC near the Atlantic shore line (left) and in MARM in the agricultural area (right).

2953

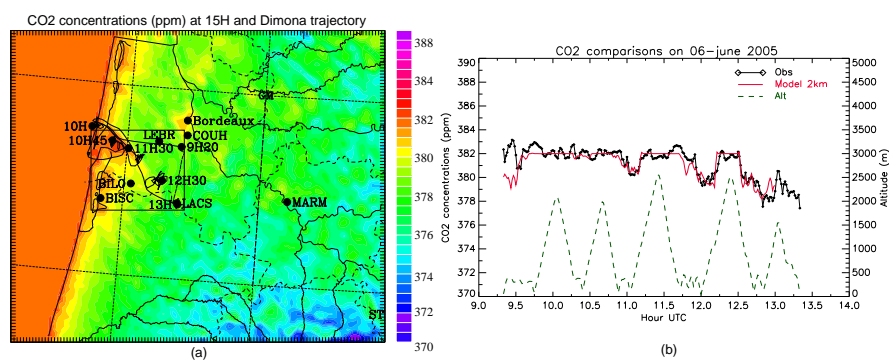


Fig. 5. (a) Simulated CO₂ concentration at 15:00 UTC and aircraft trajectory; **(b)** CO₂ concentration time series: from the model (red) and aircraft observations (black), altitude (dashed lines) during the Dimona flight over the Landes region.

2954

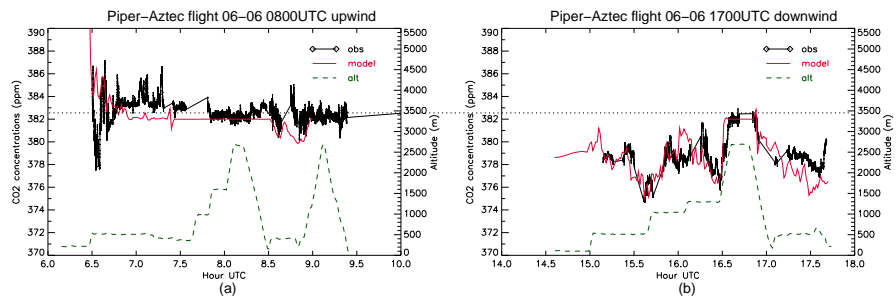


Fig. 6. CO_2 concentration time series: from the model (red) and aircraft observations (black), altitude (dashed lines). **(a)** for the upstream morning flight, **(b)** for the downstream afternoon flight.

2955

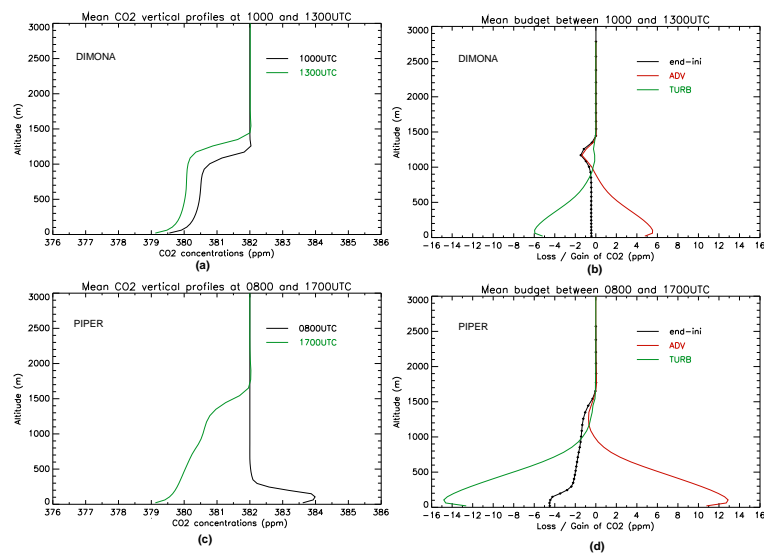


Fig. 7. Eulerian budget from the model: **(a)** averaged vertical profiles of CO_2 concentration over the Dimona sub-domain at 10:00 (black) and 17:00 UTC (green); **(c)** same than **(a)** for the Piper-Aztec sub-domain at 08:00 and 17:00 UTC; **(b)** and **(d)** averaged vertical profiles of the budget terms: turbulent tendency in green, advective tendency in red and difference between the morning and afternoon profiles in black, respectively for the Dimona and Piper-Aztec boxes.

2956

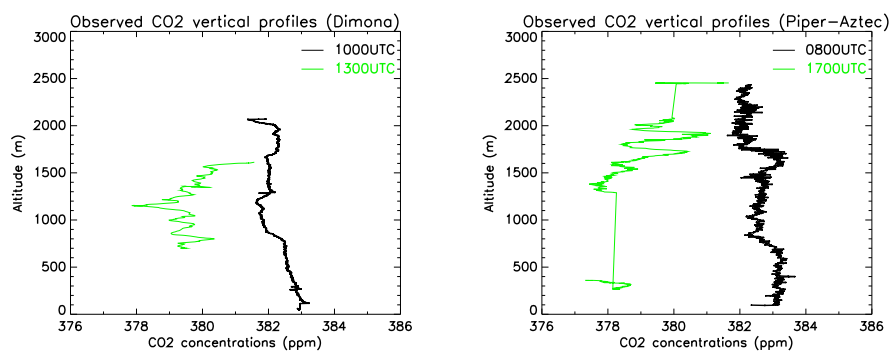


Fig. 8. Vertical profiles of CO₂ concentration observed by: the Dimona aircraft at 10:00 and 13:00 UTC (left panel) and the Piper-Aztec aircraft at 08:00 UTC and 17:00 UTC (right panel).